IOPscience iopscience.iop.org

Home Search Collections Journals About Contact us My IOPscience

Solid Kr bubbles in aluminium observed by ^{83}Kr Mossbauer spectroscopy

This article has been downloaded from IOPscience. Please scroll down to see the full text article.

1989 J. Phys.: Condens. Matter 1 1145

(http://iopscience.iop.org/0953-8984/1/6/013)

View the table of contents for this issue, or go to the journal homepage for more

Download details:
IP Address: 171.66.16.90
The article was downloaded on 10/05/2010 at 17:45

Please note that terms and conditions apply.

J. Phys.: Condens. Matter **1** (1989) 1145–1151. Printed in the UK

LETTER TO THE EDITOR

Solid Kr bubbles in aluminium observed by ^{83}Kr Mössbauer spectroscopy

G L Zhang† and L Niesen

Laboratorium voor Algemene Natuurkunde, Materials Science Centre, Westersingel 34, 9718 CM Groningen, The Netherlands

Received 11 November 1988

Abstract. We have used Mössbauer spectroscopy on the 9.40 keV transition in ^{83}Kr for the first time, in order to investigate the hyperfine interaction and lattice dynamics of Kr bubbles in Al. The spectra show two components: a single line from Kr atoms inside the bubble and a quadrupole component from Kr at the Kr–Al interface. The precipitates grow from 1.5 nm after implantation to 3.7 nm after 700 K annealing, while the characteristic Mössbauer temperature gradually decreases from 89 K to 64 K. At the same time a decrease in the isomer shift is observed. Both phenomena reflect the increase in atomic volume in the Kr bubbles during annealing. Our experiments do not show melting in the temperature range 0–230 K.

Interest in the precipitation of noble gases in metals has been stimulated by the observation of small bubbles containing noble gas atoms in the solid phase at room temperature, with corresponding pressures up to several GPa [1, 2]. Transmission electron microscopy (TEM) shows that high dose implantations of Kr in Al at room temperature lead to the formation of small solid precipitates epitaxially aligned with the Al matrix [3–5]. The molar volume found from the extra Kr reflections is 22.8 cm^3, i.e. 15% lower than the molar volume at 0 K and 1 bar. This corresponds to a pressure of 2.1 GPa at 300 K [6]. The corresponding melting temperature [7] is far above room temperature.

Mössbauer spectroscopy on the 9.40 keV transition in ^{83}Kr is a very interesting method for the study of these highly compressed precipitates. Different environments of the Kr atoms give rise to clearly different components in the spectrum. In particular, the contribution of bulk and interface atoms can be easily separated. From the relative intensities the size of the bubbles can be inferred. Moreover, the lattice dynamics can be studied directly by measuring the Debye–Waller factor (DWF) as a function of temperature, from which the characteristic Mössbauer temperature can be derived. This quantity and the isomer shift S are directly related to the atomic density in the bubbles. In this way a consistent picture of the behaviour of the Kr bubbles on annealing can be obtained.

^{83}Kr bubbles in Al were produced by ion implantation at room temperature. Al foils of thickness 1.3 μm, produced by fast evaporation, were implanted with ^{83}Kr ions with an energy of 110 keV to a total dose of 1.7×10^{16} Kr cm^{-2}. This corresponds to a local concentration of 4% in the peak of the distribution. The dose rate was $\simeq$

† On leave from Shanghai Institute of Nuclear Research, Shanghai, People's Republic of China.

0953-8984/89/061145 + 07 $02.50 © 1989 IOP Publishing Ltd

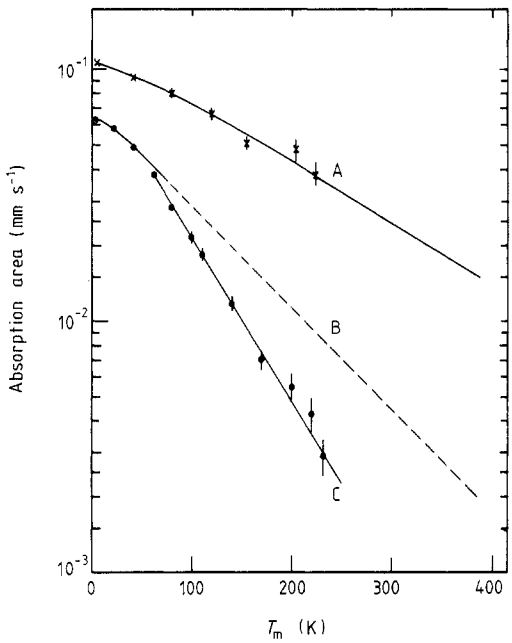

Figure 1. Mössbauer spectra taken at 4.2 K on an absorber of ^{83}Kr implanted in Al. Dose 1.7×10^{16} Kr cm^{-2}, implantation energy 110 keV. Spectra were taken directly after implantation (*a*) and after annealing for 20 min at (*b*) 533 K, (*c*) 603 K and (*d*) 700 K.

5×10^{12} Kr cm^{-2} s. A total area of 70 cm^2 was implanted at both sides, from which an absorber with 1.5×10^{18} Kr cm^{-2} was made. Assuming natural width of the absorber (0.20 mm s^{-1}), this corresponds to a Mössbauer thickness $t = 1.5$ at 4.2 K. However, the real absorber linewidth corrected for thickness effects was estimated to be two to three times larger. Consequently the area under the Mössbauer line will be proportional to the recoilless fraction of both source and absorber (thin absorber approximation).

As a source we used 0.5 mCi of ^{83}RbCl, produced via the ^{85}Rb(p, 3n)^{83}Sr reaction. A target of 750 mg cm^{-2} natural $RbCo_3$ was irradiated with 40 MeV protons to a total dose of 60 μA h, using the KVI cyclotron in Groningen. The resulting ^{83}Sr activity was chemically separated and allowed to decay to ^{83}Rb (86 d), after which a thin ^{83}RbCl source was made. Mössbauer spectroscopy was performed in transmission geometry, using a Si(Li) detector. During the measurements the source was always kept at 4.2 K, while the absorber temperature could be varied from 4.2 to 230 K. In addition measurements were performed at 4.2 K on a 2.4 mg cm^{-2} solid Kr layer adsorbed on the outer side of the Be window of the liquid helium cryostat.

The Mössbauer spectrum obtained on the as-implanted sample is displayed in figure 1(*a*). It is fitted with two components: a single line and a component split by quadrupole interaction. The latter component consists of 11 lines, the relative positions of which were calculated using $Q^*/Q = 1.958$ [8]. It was assumed that the electric field gradient V_{zz} is axially symmetric. Consequently three position parameters are necessary to fit the whole spectrum, the isomer shifts of both components and the quadrupole coupling $\Delta = eQV_{zz}$. For the single line we obtained $S = +0.029(5)$ mm s^{-1}, while for the other component we found $S = +0.017(7)$ mm s^{-1} and $\Delta = +1.83(6)$ mm s^{-1}.

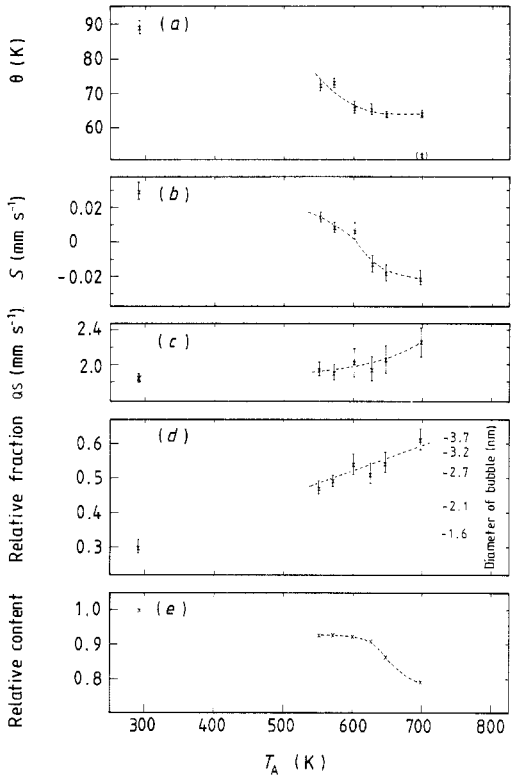

Figure 2. The behaviour of various parameters as a function of annealing temperature. (*a*) Characteristic Debye temperature: (*b*) isomer shift relative to ^{83}RbCl; (*c*) quadrupole splitting $\Delta = eQV_{ZZ}$; (*d*) relative fraction of single line; (*e*) ^{83}Kr content derived from total absorption area, normalised to value after implantation.

Some spectra obtained at 4.2 K after vacuum annealing for 20 min at various temperatures are displayed in figure 1. The linewidths did not change significantly on annealing and thereafter were kept constant at their average values 0.49(5) mm s^{-1} (single line) and 0.69(9) mm s^{-1} (quadrupole component).

The interpretation of the two components in the spectrum is straightforward. The single line is associated with atoms in the bulk of the solid precipitates, while the quadrupole component originates from atoms at the Kr–Al interface. There is no indication of the presence of a single line with $S = +0.68(3)$ mm s^{-1} that was ascribed to substitutional ^{83}Rb(Kr) atoms in Al [19]. It is well known that the EFG of atoms in the neighbourhood of a metal surface decreases from a high value at the outermost layer to nearly the bulk value in the next layer [9, 10]. Therefore we can estimate the size of the precipitates from the ratio of the areas of the two components (any difference in recoilless fraction is negligible at 4.2 K). Figure 2(*d*) displays this ratio as a function of the annealing temperature T_A. On the right-hand side the corresponding sizes are indicated. These values are calculated assuming cubic shapes with the Kr–Al interface in ⟨100⟩ planes. Such an orientation is suggested by the work on ^{111}In in Al co-implanted with noble gases [11, 12]. For other shapes or orientation of interfaces the resulting sizes will be slightly different, but the overall trend is the same: after implantation the bubbles are small

(≈1.5 nm), while on annealing they gradually grow to 3.7 nm at $T_A = 700$ K. This is in good agreement with the TEM observations [3–5] and gives additional support to our interpretation of the two components in the Mössbauer spectra. Using the density found in TEM experiments, a precipitate of 1.5 nm size would contain about 100 atoms. The pressure corresponding to this density is 1.1 GPa at 4.2 K [13], increasing to 2.1 GPa at room temperature [6].

Using $eQV_{zz} = +1.9$ mm s^{-1} we derive $V_{zz} = +2.4 \times 10^{17}$ V cm^{-2} for the interface EFG. The sign is in agreement with that for a metal–vacuum interface [14]. The value for V_{zz} should be interpreted as an average over terrace sites and various edge sites. Although the spectra have insufficient resolution to observe these sites directly, their existence is consistent with the relatively large linewidth of the quadrupole component.

Spectra were taken as a function of temperature after implantation and after each annealing step. No systematic changes in the intensity ratio of the single line to quadrupole component were found, indicating that the recoilless fraction of both components was nearly the same. The total absorption area as a function of T is shown in figure 3 for various annealing temperatures. Except for the measurements at the highest annealing temperature all data could be fitted very well assuming a simple Debye model. The resulting characteristic temperatures θ are displayed as a function of T_A in figure 2(*a*). A large decrease is observed from 89(2) K after implantation to 63.7(1.0) K after $T_A =$ 648 K. The last value is close to the value 61(2) K we measured from the absorption area of a solid Kr layer at 4.2 K and also in agreement with an earlier evaluation of low-pressure recoilless fraction data on solid Kr [15]. Essentially the same value, $\theta =$ 64.4(2.2) K, is obtained from the three lowest points ($T < 60$ K) after annealing at 700 K. In contrast, in this case the region $60 < T < 230$ K could be fitted quite well with a much lower value: $\theta = 51.6(5)$ K; see figure 3. This is practically the value of θ at the melting point at ambient pressure derived from a thermodynamic analysis [16].

In all cases the area showed a smooth dependence on T up to the highest temperatures. In particular, no drop is observed at 115.4 K, the melting temperature of Kr at 1 bar. We derive from the data that at least 90% of the Kr atoms remain in the solid phase up to 230 K, even after annealing for 20 min at 700 K. This behaviour is not surprising in view of the average size of the Kr precipitates after annealing (≈3.7 nm) and is in agreement with the electron diffraction data of Bircher and Jäger for approximately the same dose [4]. A different behaviour was found in x-ray diffraction experiments on Kr-implanted Al [17]. In this case annealing at 620 K leads to melting at 116 K of large bubbles (size ≈9 nm) containing most of the Kr atoms. The creation of these large bubbles may be associated with the different implantation conditions (dual implantation, larger dose) and the much longer anneal time [18].

In figure 2(*b*) the isomer shift of the single line at 4.2 K is plotted as a function of T_A. A gradual decrease of 0.061(6) mm s^{-1} is observed in the measured value of the isomer shift for solid Kr: $S = -0.032(2)$ mm s^{-1}. Using the known value of $\Delta\langle r^2\rangle$ for this transition [19], this corresponds to a decrease in the electron density at the nucleus of 0.51(9) a_0^{-3}. The isomer shift of the quadrupole component showed the same trend, although with larger errors.

The behaviour of the quadruple interaction constant is displayed in figure 2(*c*). It shows a slight tendency to increase as a function of T_A, possibly because during bubble growth the number of regular terrace sites will increase relative to the number of edge sites.

Finally figure 2(*e*) shows the relative Kr content derived from the total area at 4.2 K and corrected for small changes of the recoilless fraction at 4.2 K. A clear loss of Kr

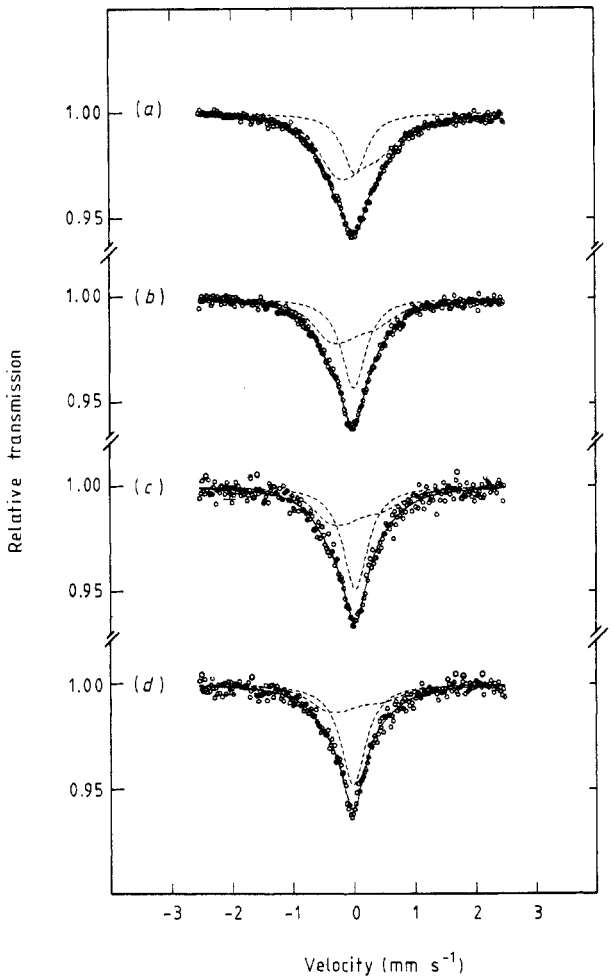

Figure 3. Total absorption area of Mössbauer spectra plotted against measuring temperature T_m, after implantation (×) and after annealing at 648 K and 700 K (●). Curves A, θ = 89.1(19) K; B, θ = 64.4(22) K; C, θ = 51.6(5) K.

atoms due to out-diffusion during annealing can be observed, but the effect remains rather small up to T_A = 700 K.

The behaviour of the various Mössbauer parameters on annealing can be understood on the basis of two phenomena: the size of the precipitates increases and the density in the precipitates decreases. Unlike in the TEM experiments, distinct irreversible changes are observed already after annealing at 553 K, which is 59% of the melting temperature of Al. At a comparable Kr dose the TEM experiments observe melting of the precipitates around 620 K, i.e. 66% of the melting temperature T_m. The situation is quite different from that in the FCC metals Cu and Ni where melting [20] and a decrease of the Kr density [21] is observed around 40% of the melting point of the host metal. In our case the first stage of bubble growth is probably governed by trapping of thermally created vacancies. This mechanism should become operative around 0.5 T_m, i.e. 470 K for Al. In this way the internal pressure in the bubble can reach equilibrium with the surface tension in the

Table 1. Parameters of Mössbauer spectra taken at 4.2 K on a sample of ^{83}Kr in Al. S_1 and S_2 are the isomer shift of the single line and quadrupole component respectively. Δ_2 is the quadrupole coupling constant.

T_A (K)	S_1 (mm s^{-1})	S_2 (mm s^{-1})	Δ_2 (mm s^{-1})
293	0.029(5)	0.017(7)	1.83(6)
553	0.014(3)	−0.06(1)	1.94(8)
573	0.008(3)	−0.06(1)	1.90(9)
603	0.006(5)	−0.04(2)	2.21(17)
628	−0.13(5)	−0.06(1)	1.94(14)
648	−0.018(5)	−0.04(2)	2.05(16)
700	−0.021(4)	−0.07(3)	2.27(19)

Al interface. For a spherical bubble this would mean: $p = 2\gamma/r$, where γ is the surface energy density ($\simeq$1 N m^{-1} for Al) and r the bubble radius. Apart from the numerical constant this equation also holds for other shapes. Combination with the EOS of Kr [6] leads to the conclusion that in this mechanical equilibrium regime an increase in the temperature leads to an expansion of the bubble and a corresponding slight decrease of the bubble pressure. This is a reversible process as long as the total number of Kr atoms in the bubble remains constant. However, at the same time bubbles will grow by agglomeration of Kr atoms. The corresponding increase in size leads to a lower equilibrium pressure and density in the bubble.

Cooling after annealing then leads first to a small increase in pressure, down to the temperature where individual vacancies can no longer escape from the precipitate. Below this vacancy freezing temperature T_V the density in the bubble is constant, apart from a small effect from the host lattice. Our recoilless fraction measurements are performed in this regime. This explains why the Debye model yields such a good description of these measurements: at constant molar volume the phonon spectrum will change only slightly with increasing temperature and the characteristic temperatures of the phonon spectrum, $\theta(n) \equiv (\hbar/k_B)[(n+3)\mu(n)/3]^{1/n}$ with $\mu(n) = \int \omega^n g(\omega)\, d\omega$, will stay practically constant. The recoilless fraction is determined by $\theta(-1)$ at low T and by $\theta(-2)$ for $T \geqslant \theta(-2)$. The success of the Debye model in this case implies that $\theta(-1) \simeq \theta(-2)$.

The dependence of θ on the molar volume V_m is given by $\theta \simeq V_m^{-\gamma}$, where γ is the Grüneisen constant. Combining our data on θ with the TEM data on V_m we get $\gamma = 1.9(2)$. This value is somewhat lower than derived from MD calculations using a 12/6 Lennard-Jones potential [22]. Similar calculations using the accurate BWF Kr potential [23] would be highly desirable.

Only after annealing at 700 K does the recoilless fraction not fit the Debye model. The reason may be that after this anneal the molar volume at T_V is higher than 27.1 cm^3, the value for solid Kr at 1 bar. In that case the Kr precipitate can freely expand up to $\simeq$60 K, above which the volume is limited again by the nearly constant volume of the Al cavity, leading to a constant, but lower, value of θ.

For the case of Kr the Lindemann criterion for melting can be written as $\langle x^2 \rangle_M^{1/2} = 0.115 R_{NN}$ where $\langle x^2 \rangle_M^{1/2}$ is the RMS amplitude of the Kr atoms and $R_{NN} = 0.412$ nm is the nearest neighbour distance, both taken at the melting point T_m [16]. For the as-implanted

sample we obtain $T_m \simeq 680$ K by extrapolation of our recoilless fraction data. In practice the start of the melting of bubbles is observed by TEM at a somewhat lower temperature (620 K), because some bubble growth and decrease of Kr density takes place already before the melting point is reached. The Lindemann criterion combined with our data predicts that after annealing at 700 K melting starts at $\simeq$230 K, i.e. at the highest measurement temperature. This is still twice the melting temperature at ambient pressure. We conclude that this criterion, which works well in the case of bulk rare gases, yields estimates consistent with the experimental data.

In conclusion, we have shown by ^{83}Kr Mössbauer spectroscopy that after implantation of $\simeq$4% Kr in Al the large majority of the Kr atoms are aggregated in bubbles with an average size of 1.5 nm. The recoilless fraction of the Kr atoms can be described very well with a Debye model. On annealing, the size of the bubbles increases gradually, with an accompanying increase in the molar volume. No melting is observed up to 230 K, even after annealing at 700 K.

We want to thank the technical staff of the KVI in Groningen and F Th ten Broek for their help in producing the ^{83}RbCl source. The implantations were performed under the guidance of J J Smit. We acknowledge useful discussions with Professor Dr J Th M de Hosson, Dr A van Veen and Dr E Johnson. This work was performed as part of the research programme of the Stichting voor Fundamenteel Onderzoek der Materie (FOM) with financial support from the Nederlandse Organisatie voor Wetenschappelijk Onderzoek (NWO).

References

[1] vom Felde A, Fink J, Müller-Heinzerling Th, Pflüger J, Scheerer B, Linker G and Kaletta D 1984 *Phys. Rev. Lett.* **53** 922
[2] Templier C, Jaouen C, Rivière J-P and Grilhè J 1984 *C. R. Acad. Sci., Paris* **299** 613
[3] Birtcher R C and Jäger W 1986 *Nucl. Instrum. Methods* B **15** 435
[4] Birtcher R C and Jäger W 1987 *Ultramicroscopy* **22** 267
[5] Hashimoto I, Yorikawa H, Mitsuya H, Yamaguchi H, Takaishi K, Kikuchi T, Furuya K, Yagi E and Iwaki M 1987 *J. Nucl. Mater.* **149** 69
[6] Ronchi C 1981 *J. Nucl. Mater.* **96** 314
[7] Crawford R K and Daniels W B 1971 *J. Chem. Phys.* **55** 5651
[8] Holloway J H, Schrobilgen G J, Bukshpan S, Hilbrants W and de Waard H 1977 *J. Chem. Phys.* **66** 2627
[9] Schatz G private communication
[10] Korecki J and Gradmann M 1985 *Phys. Rev. Lett.* **55** 2491
[11] Pleiter F, Post K, Mohsen M and Wieringa T S 1984 *Phys. Lett.* **101A** 363
[12] Schumacher R and Vianden R 1987 *Phys. Rev.* B **36** 8258
[13] Anderson M S and Swenson C A 1975 *J. Phys. Chem. Solids* **36** 145
[14] Lindgren B 1987 *Hyp. Int.* **34** 217
[15] Kolk B 1971 *Phys. Lett.* **35A** 85
[16] Crawford R K 1977 *Rare Gas Solids* vol II, ed. M L Klein and J A Venables (London: Academic) p 771
[17] Andersen H H, Bohr J, Johansen A, Johnson E, Sarholt-Kristensen L and Surganov V 1987 *Phys. Rev. Lett.* **59** 1589
[18] Johnson E private communication
[19] Spijkervet W J J, Pleiter F and de Waard H 1980 *Hyp. Int.* **8** 173
[20] Evans J H and Mazey D J 1985 *J. Phys. F: Met. Phys.* **15** L1
[21] Jensen K O, Eldrup M, Pedersen N J and Evans J H 1988 *J. Phys. F: Met. Phys.* **18** 1703
[22] Dickey J M and Paskin A 1969 *Phys. Rev.* **188** 1407
[23] Barker J A, Watts R O, Lee J K, Schäfer T P and Lee Y T 1974 *J. Chem. Phys.* **61** 3081